

This document is downloaded from DR-NTU, Nanyang Technological University Library, Singapore.

Title	Residual stress study of welded high strength steel thin-walled plate-to-plate joints, part 1 : experimental study
Author(s)	Lee, Chi King; Chiew, Sing Ping; Jiang, Jin
Citation	Lee, C. K., Chiew, S. P., & Jiang, J. (2012). Residual stress study of welded high strength steel thin-walled plate-to-plate joints, Part 1: Experimental study. <i>Thin-Walled Structures</i> , 56, 103-112.
Date	2012
URL	http://hdl.handle.net/10220/18895
Rights	© 2012 Elsevier. This is the author created version of a work that has been peer reviewed and accepted for publication by <i>Thin-Wall Structures</i> , Elsevier. It incorporates referee's comments but changes resulting from the publishing process, such as copyediting, structural formatting, may not be reflected in this document. The published version is available at: [DOI: http://dx.doi.org/10.1016/j.tws.2012.03.015].

Residual stress study of welded high strength steel thin-walled plate-to-plate joints, Part 1: Experimental study

*C. K. Lee, S. P. Chiew and Jin Jiang

School of Civil and Environmental Engineering

Nanyang Technological University

50 Nanyang Avenue, Singapore 639798

*Email: ccklee@ntu.edu.sg

ABSTRACT

In this study, an investigation on the residual stress distributions near the weld toe of high strength steel thin-walled plate-to-plate T and Y-joints is carried out. Two groups of specimens, corresponding to welding performed at ambient temperature and at a preheating temperature of 100°C, are fabricated. The effects of preheating and joint geometry on the residual stress distribution near the weld toe are investigated by using the ASTM hole-drilling method. Furthermore, a study is also performed to evaluate the influence of brace plate cutting on the residual stress distribution near the weld toe of the joints. Experimental results obtained shown that tensile residual stress up to one third of the yield strength could appear near the weld toe and its value increases as the plate thickness and intersection angle increase. Furthermore, preheating was found to be an effective way to reduce the magnitude of residual stress while brace plate cutting could release the residual stress along the weld toes significantly.

Keywords: Residual stress distribution, high strength steel, thin-walled plate-to-plate T and Y-joints, The ASTM hole-drilling method.

1. INTRODUCTION

Currently, most steel structures are made of mild steel for its satisfactory mechanical property and availability. In existing codes of practice, mild steel is well specified for structural application [1]. However, for its higher strength to weight ratio, recently there has been an increasing interest in the use of high strength steel (HSS) with yield strength larger than 460MPa. Compared with mild steel, HSS has merits in economy, aesthetics and safety. However, the stress-strain behaviour of HSS is different from mild steel such that HSS exhibits reduced ductility. Furthermore, residual stress due to welding in HSS could be more serious than that in mild steel and might have a negative impact on its fatigue performance. It is found that the effect of residual stress on the performance of welded HSS connection is particularly significant if the nominal stress is low [2] when comparing with the yield stress of the materials. Hence, a good understanding of residual stress distribution around welded intersection is important when assessing the mechanical performance of HSS structures.

Many researchers have shown their interests in HSS since the 1990s [3-9]. While Chen [10] proposed that the parent steel grade does not have obvious influence on fatigue life. However, such conclusion was based on unwelded details or welded details with special treatment during welding. The use of HSS may be of advantage when the expected number of nominal load cycles is comparatively small or when the mean stress is high so that the fatigue strength is not the dominating design factor [11]. Anami and Miki [12, 13] reviewed development and the use of HSS for bridge structures in Japan. It was found that the most important issue for the application of HSS is to achieve a balance between tensile strength and fatigue performance without losing good weldability. Up to now, the effect of residual stress in HSS connection is not well understood. However, it is well accepted that as the strength level of steel increases, it becomes

more difficult to weld without cracks and other defects. In addition, HSS can tolerate lesser defects since they are less ductile and more sensitive to stress corrosion cracking and hydrogen embrittlement [14]. Maddox proposed [11] that the magnitude of residual stress increases with the material yield strength and a higher residual stress in welded HSS connection could lead to a reduction in fatigue strength when compared with welded mild steel connection. Stacey and Barthdemy [15] incorporated the effects of residual stress into their suggested structural integrity assessment procedure. Billingham et al. [16] and Bjorhovde [17] summarized some aspects for the use of HSS and gave a brief discussion on the influence of residual stress. Masubuchi and Martin [18, 19] investigated residual stress in butt welds in low carbon steel and in quenched and tempered steel. Lee et al. [20] investigated the effect of residual stress on component failure for T-plate and tubular T-joint. Recently, Acevedo and Nussbaumer [21] studied the residual stress distribution of welded tubular K joints near the weld toe. They assumed that when the standard ASTM hole-drilling strain gauge method [22] is employed for residual stress measurement, the residual stress distribution measured near the weld toe will not be affected when the brace of joint was cut off to facilitate the measurement procedure.

Despite that some understanding has been gained on the impact of residual stress on mild and alloyed steel, relatively little information is available on its distribution in HSS thin-walled connections. In particular, majority of the previous studies was focused on the residual stress distribution in transverse butt welds rather than on load carrying welded joints. The main objective of the current study is to carry out an investigation on the residual stress distributions in load carrying welded HSS thin-walled plate-to-plate T and Y- joints. In particular, the influences of the joint geometry and the impacts of preheating during the welding are investigated. The whole study will be reported in two parts. In Part I, details of an experimental study which was

carried out to explore the residual stress distribution near the weld toes for different small size HSS joints are given. In Part II [23], focus is given to the development and verification of a proper numerical modeling procedure of the welding process. In addition, based on the verified numerical model, a parametric study is carried out to investigate the impacts of some key welding parameters on the resulted residual stress distributions.

In the next section, a brief review of the standard ASTM hole-drilling method for residual stress measurement [22] and some important details of the specimen fabrication are presented. The details of the experimental set up such as the strain gauge scheme employed are then given in Section 3. In Section 4, the results of the experimental study including the effects of preheating and other key geometrical parameters on the residual stress distribution are reported. Finally, conclusions for this part of the study are presented.

2. THE ASTM HOLE-DRILLING METHOD AND SPECIMEN SPECIFICATIONS

2.1 The standard ASTM hole-drilling method

The standard ASTM hole-drilling method [22] is a common way for measuring residual stress by removing localized stress and measuring strain relief in the adjacent material. It causes relatively little damage to the specimen (as drilling is limited to 1-2 mm on the surface of the specimen [22]) and allows localized residual stress measurements. The principle of the method is to release the localized stress by introducing a small hole into a residually stressed structure and thus changing the local strain on the surface of the testing. By comparing the stress at this point before and after hole-drilling, stress relaxation due to hole drilling can be determined. On the assumption that the material of the plate is homogenous and isotropic and its stress-strain curve

is linear, the relieved strain at a point $P(R, \alpha)$ can be obtained by substituting the stress relaxation into the Hooke's law [22]

$$\varepsilon = \frac{1+\nu}{E} \cdot \bar{a} \cdot \frac{\sigma_x + \sigma_y}{2} + \frac{1}{E} \cdot \bar{b} \cdot \frac{\sigma_x - \sigma_y}{2} \cos 2\alpha + \frac{1}{E} \cdot \bar{b} \cdot \tau_{xy} \cdot \sin 2\alpha \quad (1)$$

In Eqn. 1, E is the Young's modulus, ν is the Poisson's ratio and ε is the relieved strain. σ_x and σ_y are the stresses in the x and the y directions respectively. α is the angle from the x -axis to the maximum principle stress (Fig. 1). \bar{a} and \bar{b} are calibration constants. In residual stress measurement, after the three groups of relieved strains are obtained by a strain rosette, σ_x , σ_y and α can be determined.

2.2 Specimen specifications

In the present experimental investigation, a number of thin-walled plate-to-plate T and Y joints, made of HSS plate with minimum yielding stress of 690MPa, were fabricated by shielded metal arc welding (SMAW). The RQT701 HSS plate used in this study is quenched and tempered structural steel with improved forming and welding performance by substituting some alloying element with carbon [24]. In order to prevent hydrogen cracking for the HSS plate, an ultra low hydrogen and moisture resistant type covered electrode for low temperature service, LB-70L, which is equivalent to the class AWS A5.5 E10016-G and supplied by Kobelco of Japan [25] was used. The diffusible hydrogen content of this electrode is 4ml/100mg. Table 1 gives the mechanical properties of the steel plate and the electrode. Table 2 lists the chemical composition of the RQT701 steel plate and the LB-70L electrode employed in this study.

In order to compare the influence of preheating on residual stress distribution near the weld toe, two groups of specimens were prepared. In the first group, all welding steps were performed at

ambient temperature (30°C). All specimens from the second group were preheated before welding. Following the recommendation from the EN1011-2:2001[26], the minimum preheating temperature T_p is depended on the equivalent carbon content CET , the plate thickness d , the hydrogen content of the weld metal HD and the heat input Q , and could be calculated as

$$T_p = T_{pCET} + T_{pd} + T_{pHD} + T_{pQ} \quad (2)$$

$$\begin{cases} T_{pCET} = 750 \times CET - 150 \\ T_{pd} = 160 \times \tanh(d / 35) - 110 \\ T_{pHD} = 62 \times HD^{0.35} - 100 \\ T_{pQ} = (53 \times CET - 32) \times Q - 53 \times CET + 32 \end{cases} \quad (3)$$

In Eqns. 2 and 3, the unit of the temperature is in degree Celsius (°C). T_{pCET} , T_{pd} , T_{pHD} and T_{pQ} are respectively the preheat temperatures corresponding to the equivalent carbon content, the plate thickness, the weld metal hydrogen content and the heat input. By using the data given in Tables 1 and 2, the recommended minimum preheating temperatures for joints with 8mm, 12mm and 16mm RQT701 steel plate were found to be equal to 76°C, 85°C and 94°C, respectively. However, in order to make the fabrication procedure easy to handle, a single preheating temperature of 100°C was applied to all preheated joints.

For each group of the specimen, there are six different geometries, consisting of three different plate thicknesses (8mm, 12mm and 16mm) and two joint intersection angles (90° and 135°). All joints were fabricated by a qualified welder using hand welding. For the 90° joint, two sets of duplicated specimens with the same welding procedure and joint geometry were fabricated to assess the effects of brace plate cutting (see Section 3.5 for more details). Hence, in the experimental study, a total of 18 joints were produced and tested. Fig. 2 shows the typical specimen cross-sectional geometry and the welding profile of the joint while Table 3 lists the geometry of the specimens. Note that the width of all specimens fabricated is equal to 150mm.

As shown in Fig. 2, in a typical welding procedure, a T or Y joint was formed by adding the welding filler (region $I-J-G-H$ in Fig. 2) from the surface $H-G$, where it was packed by ceramic plate and ended at the surface $I-J$. The plate $A-B-C-D$ and the plate $E-F-G-J$ are named as the *chord plate* and the *brace plate*, respectively. θ and β are the joint intersection and the end preparation angles respectively. l_1 and l_2 are respectively the length of chord and brace plates while t_1 and t_2 are their thicknesses. R is the weld root opening distance.

2.3 Welding Specification

In this study, all full penetration welding profiles created for the plate-to-plate joints are complied with the AWS D1.1 2008 [27] guideline. Table 4 lists the welding parameters for the fabrication. Before the welding started, the surfaces of the chord and brace plates were cleaned so that the specimens were free from slag and rust. It was then followed by end preparation. To avoid distortion and shrinkage, several splices were welded to assemble the chord and brace plates together. In the process of preheating, the area close to where the weld filler was added (Fig. 3 and Fig. 4) was heated up to 100 °C. Temperature chalk was employed to ensure the preheating temperature was reached. As in the second part of the current study [24], numerical modeling will be carried out to study the effects of the number of weld passes and welding sequence on the residual stress distribution, the number of weld passes and the welding sequence employed during the fabrication were carefully recorded. For 135° joints, 9, 14, 22 welding passes were employed for joints with plate thickness of 8mm, 12mm and 16mm, respectively. For 90° joints, 11, 13, and 17 welding passes were used for joints with plate thickness of 8mm, 12mm and 16mm, respectively. Fig. 5 shows the number of weld passes and the welding sequences adopted for different joint angles and plate thickness. Given that the width

of all specimens is equal to 150mm, with an average welding speed of 2.6mm/s, the time interval between each weld pass is roughly equal to 58s. Thus, the temperature in the weld filler after finishing a weld pass shall still be higher than 100°C. Hence, for all specimens preheating was only conducted before the first weld pass but was not repeated between successive passes.

3. EXPERIMENTAL INVESTIGATION

3.1 Setup and modification of the hole-drilling guide

The RS-200 Milling Guide, a high-precision instrument for residual stress analysis by the hole-drilling method through drilling of a hole in the centre of a special strain gauge rosette, was used for measuring the residual stress in the specimens. The original form of the milling guide is shown in Fig. 6(a). However, a physical limitation exists in the original setup: The journal hole fixing the high-speed air turbine is positioned at the centre of the triangular base of the milling guide. As a result, there exists a minimum offset distance of 50mm between the edge of the guide base and the position of the drilled hole (centre of the strain gauge). As the bracing plate of a 90° joint will obstruct the guide base, such constraint greatly handicaps the original guide's usage in this study. To overcome such problem, an improved set up was designed and fabricated as shown Fig. 6(b). In order to move the measurement point closer to the weld toe of the joint, the original triangular base was replaced by a tailor-made trapezoidal base supported by three swivel pads. Furthermore, the cylinder housing the journal was further machined down to reduce the minimum distance between the drilled hole and the guide base edge to 10mm.

3.2 Strain gauge locations

A special type of strain rosette FRAS-2, which is specially designed so that the three strain gauges (Grids 1, 2 and 3 in Fig. 1) are all positioned on one side of the measurement point, is used to measure the released strain of the specimen during drilling. The strain gauge scheme employed for residual stress measurement on *the chord plate* is shown in Fig. 7. For 135° joints, along the longitudinal direction (the x axis in Fig. 7), three strain gauges A , B and C were placed at 5mm from the weld toe (i.e. $y=5\text{mm}$ at Fig. 7, which is corresponding to approximately 10mm from the guide base edge) with $x=25\text{mm}$, 75mm and 125mm , respectively. In addition, at the middle of the plate width where $x=75\text{mm}$, another two strain gauges B_1 and B_2 were placed at where $y=20\text{mm}$ and 35mm , respectively. The strain gauge setting for the 90° was similar to the case of 135° joints excepted that gauges A and C are removed and an addition gauge B_3 was placed at the middle of plate width with $x= 50\text{mm}$.

3.3 Calibration test for residual stress measurement

To ensure the accuracy of the residual stress measurement of the joints, a calibration test was performed to determine the coefficients \bar{a} and \bar{b} in Eqn. (1). It is accomplished by using a small size (200mm×70mm) calibration plate which was cut out from the same batch of RQT701 steel plate used for joint fabrication. The calibration plate was fixed on a tensile machine and a strain gauge rosette was placed and oriented in such a way that Grid 1 and Grid 3 (Fig. 1) were parallel to the loading direction the transverse axis, respectively. Before hole-drilling, a small calibration loading P_c was applied to develop the desired uniform calibration stress σ_c which is much less than the yield stress of the plate. The values of relieved strain from Grid 1, ε_1' , and Grid 3, ε_3' , were then recorded. The loading was then released and the calibration plate was removed from

the tensile machine. A standardized hole with depth equals to 2 mm was drilled and the specimen was then remounted to the tensile machine. The same calibration loading P_c was re-applied and the corresponding Grid 1 and Grid 3 strains ε_1' and ε_3' were recorded. To make the results more reliable, eight groups of readings were recorded to obtain coefficients \bar{a} and \bar{b} that are required by the ASTM standard [23] at different depths ranging from 0 to 2mm with 0.25mm steps. Table 5 lists the values of the calibration coefficients obtained for different depths.

3.4 Residual stress measurement at a selected point

For the residual stress measurement at a selected point, before mounting the strain gauge, a pair of crossed reference lines were first marked on the surface at where strain measurement were needed. Careful alignment of the milling guide with the strain gauge hole centre with a precision within 0.025mm was accomplished by inserting a special-purpose microscope into the guide's centre journal, and then positioning the guide precisely over the centre of the rosette. A 1.6mm diameter tungsten carbide cutter was installed in the turbine. The milling cutter was guided precisely during the drilling operation to ensure that the cutter progress in a straight line during drilling. Finally, a hole with depth equal to 2 mm was bored by setting the compressed air supply to the high-speed turbine to produce a circular, straight-sided and flat-bottomed hole. The hole should first be advanced slowly to a depth $0.05D$ (D is the diameter of gauge circle that is shown in Fig. 1. The actual size of D is 5mm) and the relieved strain was noted. The drilling and strain measurement steps were then repeated for seven times with an incremental depth of $0.05D$ until a final hole depth approximately equal to $0.4D$ (2 mm) was achieved. The residual stress at that point is then calculated by using the averaging method which is suggested by the ASTM guide

[22]. The averaging method uses all 8 groups of measured data to reduce the effects of random strain measurement.

3.5 Cutting of brace plate

Despite that in the current study the milling guide was modified to allow residual strain measurement to be carried out at location as close as 5mm from the weld toe of plate-to-plate joints with $\theta \geq 90$, the same set up is not applicable to joints with $\theta < 90$ or other joint type such as circular hollow section joints. In such cases, researchers may resolve to the method of brace cutting [21] in which the brace plate obstructing the drill is removed (either by flame or mechanical cutting) to facilitate residual stress measurement near the weld toe. However, so far little information is available on the effect of brace plate cutting operation on the residual stress distribution near the weld toe. Hence, in this study an investigation was conducted to study the effect of brace plate cutting. The brace plates of half of the 90° joints fabricated were mechanically cut before the residual stress measurement were conducted (Table 6, the fourth column). The cutting position was chosen to be a surface 5mm above the weld toe at the brace plate. Figs. 8 and 9 show a T-joint before and after brace plate cutting, respectively

4. EXPERIMENTAL RESULTS

The measured residual stresses obtained from the experimental study are listed in Table 6. In the next five sections, results related to the distribution of residual stress along the weld toe, the effects of preheating, joint angle, plate thickness and brace plate cutting are presented.

4.1 Distribution of residual stress along the weld toe

From the results shown in Table 6 for gauges *A*, *B* and *C* for 135° joints, it can be seen that for both joints with and without preheat treatment, the residual stresses at the two ends of joint (gauges *A* and *C*) are considerably less than that at the middle (gauge *B*). Furthermore, in some cases, even compressive residual stresses were recorded at gauges *A* and *B*. Such distribution of residual stress along the weld toe (*x* axis of Fig. 7) is obviously due to the boundary effects at the two ends of the joint. Since the two ends of the joint were free from any in-plane restraint, the magnitude of the residual stress is much smaller than that at the middle of the joint. As a result, in the next four sections, focus will be given to the variation of residual stress along the transverse direction (*y* axis in Fig. 7) at the middle of the joint (gauges *B*, *B1*, *B2* and *B3*).

4.2 The effects of preheating

Fig. 10 shows the residual stress distribution along the transverse direction (*y* axis) for 90° joints. Six curves are plotted to compare the preheating effect on residual stress distribution for different plate thicknesses. At gauge *B* (5mm from weld toe), the maximum residual stress for joints without preheating treatment exceeds 100MPa (roughly 1/6 of the yield strength). In addition, it can be seen that the residual stress for all preheated joints are less than their ambient counterparts (65.3%, 32% and 16.6% reductions for 8mm, 12mm and 16mm joints, respectively). Such stress relieving benefit can still be observed at gauge *B1* (20mm from the weld toe) and gauge *B2* (35mm from weld toe). The only exception occurred for the 8mm joint at gauge *B1* where the residual stress for preheated joint is 24.2% higher than its ambient counterpart. At gauge *B3* (50mm from weld toe), it appears that the effect of preheating was not significant.

Fig. 11 shows the residual stress distribution along the transverse direction (y axis) for 135° joints. Again, six curves are plotted to compare the preheating effect on residual stress distribution for different plate thicknesses. From Fig. 11, it can be seen again that at 5mm from the weld toe, the maximum residual stress without preheating treatment exceeds 200MPa (roughly 1/3 of yield strength) and preheating effectively relieved the magnitude of the residual stress (21.1%, 38.8% and 37.8% reductions for 8mm, 12mm and 16mm joints, respectively). Similar to 90° joints, at gauges B1 and B2 the relieving effect of preheating was reduced when comparing with gauge B.

From Table 6 and Figs. 10 and 11, it can be concluded that the magnitude of residual stress is highest near the weld toe (especially for the joints without preheating). Furthermore, in general, the residual stress magnitude decreases nonlinearly as the distance from the weld toe increases. When the distance exceeds 50mm, the residual stress fluctuates around zero. Regarding the preheating effect on the distribution of residual stress, it was shown that preheating could effectively reduce the magnitude of the residual stress near the weld toe (within 5mm) for both 90° and 135° joints. However, the stress relieving effects due to preheating reduces as the distances from the weld toe increases.

4.3 The effects of joint angle

Fig. 12 shows the residual stresses distributions along the transverse (y axis) for 90° and 135° joints welded at ambient temperature. From Fig. 12, it can be seen that at gauge B (5mm from weld toe) residual stress for 135° joints is higher than in that for 90° joints for all thickness (the differences are 40.9MPa, 14.8MPa and 98.1Ma for 8mm, 12mm and 16mm joints, respectively). However, at gauge B1 (20mm from weld toe) and gauge B2 (35mm from weld toe), while the

magnitude of residual stress for 135° joints is still higher than 90° joints, the effect of the welding angle is less significant.

Fig. 13 shows the residual stresses distributions along the transverse (y axis) for 90° and 135° joints welded with preheating. Similar to the case of joint welded in ambient temperature, the residual stresses for 135° joints are higher than that for 90° joints with most noticeable difference at gauge B.

The effect of joint angle on the residual stress observed from the experimental study could be explained by considering the interrelationship and the influence of weld geometrical size and the difference of heat input (the energy transferred per unit length of weld). It can be seen in Fig. 5 that the number of weld passes and, more importantly, the amount of welding material added to the joint (the weldment) required to form a 135° joint is more than that for a 90° joint. This obviously means that more heat energy was input to the 135° joint. In addition, a bigger weldment also implies that a bigger molten pool and a bigger heat affected zone should be formed during the welding of the 135° joint. Hence, even when one assumes that the cooling rate for 90° and 135° joints is the same, higher residual stress is eventually generated in the 135° joints.

4.4 The effects of plate thickness

From Figs. 10 to 13 and Table 6, it can be seen that for both 135° and 90° joints, in general, higher residual stress was found for joints fabricated with 16mm plates, regardless whether the joint was preheated or not. However, it should be pointed out that at gauge B, the residual stress does not always reduce as the plate thickness of the joint decreases. In fact, Table 6 indicates that in many cases (e.g. for both 90° and 135° joints welded at ambient temperature), the residual

stress at gauge B of 8mm joint could be higher than that of 12mm joint. Such observation could be explained by the fact that for very thin (e.g. 8mm) plate, while the temperature distribution generated by the welding process will be more uniform due to the small plate thickness, the joint will be cooled down more rapidly (by convection with surrounding air) due to its larger surface area to volume ratio. As the thickness of plate increases, while the temperature gradient will be increased, the cooling rate will be reduced, too. Hence, it is possible that at certain thickness (e.g. 12mm), the residual stress could attain a minimum as the reduction of the cooling rate could over-compensate the increases in temperature gradient. Finally, as the plate thickness is further increased, the temperature gradient will be increased continuously while the cooling rate will become steady (mainly contributed by conduction through the plate) and thus the residual stress will be increased again.

Regarding the effect of preheating on the residual stress range for joints with different plate thickness, for 90° joints welded at ambient temperature at gauge B, the residual stress range for joints with difference thickness is 28.3MPa (from 87.2MPa for 12mm joint to 115.5MPa for 16mm joint) while the corresponding range for preheated joints is 37MPa (from 59.3MPa for 12mm joint to 96.3MPa for 16mm joint). For the case of 135° joint, the corresponding stress ranges for joints with and without preheating treatment are 70MPa and 111MPa, respectively. Hence, it can be seen that preheating seems to be more effective to reduce the effects of plate thickness for joints with larger intersection angle.

4.5 The effects of brace plate cutting

Fig. 14 compares the effects of brace plate cutting on the residual stress distribution along the transverse direction (y axis of Fig. 7) for 90° joints welded at ambient temperature. From Fig. 14,

it can be seen that at gauge B (5mm from weld toe) the magnitude of residual stress for joints without brace cutting is much higher than that with brace plate cutting. In fact, when the brace plate was cut off, compressive stress as high as 70.3MPa was generated at gauge B. The differences in residual stresses at gauge B for 8mm, 12mm and 16mm joints with and without brace plate cutting are 180.4MPa, 96MPa and 90.6MPa, respectively. The corresponding differences are found to be reduced to 68.2MPa, 5.0MPa and 34.1MPa at gauge B1 (20mm from weld toe). It is also observed that for the joints with brace plate cutting, the maximum stress value occurs at gauge B1 instead of gauge B. However, for the joints without brace plate cutting, the maximum stress value exists at gauge B for all different plate thicknesses.

Fig. 15 compares the effects of brace plate cutting on the residual stress distribution along the transverse direction (y axis of Fig. 7) for 90° joints welded with preheating treatment. From Fig. 15, one can again observe that with brace plate cutting, the magnitude of residual stresses at gauge B are much lower than the corresponding joints without brace plate cutting. In addition, the effect of brace plate cutting also reduces as the distance from the weld top increases.

Based on the results presented in Figs. 14 and 15, it could be concluded that brace plate cutting could greatly disturb the residual stress distribution near the weld toe of the *chord plate*. Note this finding agrees with works by Law et al. [28] which also showed that the residual stress in the range of 15mm from the cutting surface was relieved for butt weld in a plate. Even though the above conclusion was based on the results obtained from plate-to-plate T joints with mechanical cutting close to the welding part, it indicates that mechanical cutting close to the welding part should be discouraged if one plans to conduct residual stress measurement near the weld toe.

6. CONCLUSIONS

In this paper, results of a carefully design experimental study conducted to investigate the residual stress distribution along the weld toe of high stress steel (HSS) thin-walled plate-to-plate T/Y joints were presented. Two sets of HSS plate-to-plate T/Y joints with different geometrical details were fabricated with and without proper preheating treatment. The standard ASTM hole-drill method was then employed to measure the value of residual stress at critical location of the joint near the weld toe. In addition, the effects brace plate cutting on the residual stress distribution was also studied. The experimental results indicated that while tensile residual stress with magnitude as high as one third of the yield strength of HSS could appear near the weld toe of the joint, proper preheating could significantly reduce the magnitude of the residual stress. It is also found that the magnitude of residual stress increases as the plate thickness and the intersection angle of the joint increase. Furthermore, the magnitude of the residual stress reduces nonlinearly as the distance from the weld toe increases. By comparing the measurement results obtained from thin-walled plate-to-plate T joints with and without brace plate cutting, it was found that any mechanical cutting operation near the welding part of a joint could considerably disturb the residual stress distributions along the weld toes.

In Part II, the results obtained in this paper will be employed to validate a numerical model for the stimulation of the welding process. After the accuracy and reliability of the numerical model is confirmed, it is then employed to carry out a parametric study to investigate the influences of different welding parameters including mechanical boundary condition, preheating temperature, number of weld passes, welding speed and welding sequence on the magnitudes and distributions of residual stress near the weld toe of HSS plate-to-plate joints.

Acknowledgment: The financial support of the Regency Steel Asia to the authors is gratefully acknowledged. The helps from Yongnam Pte Ltd. and Construction Technology Lab for the fabrication of the joints are also appreciated.

REFERENCES

- [1] BSI. Eurocode3: Design of steel structures. Part1-1: General rules and rules for buildings. London, UK, British Standards Institute, 1995.
- [2] Mattias Clarin. High strength steel local buckling and residual stresses. Department of Civil and Environmental Engineering. Lulea, Lulea University of Technology. Licentiate, 2004.
- [3] Healy J, Billingham J. Metallurgical considerations of the high yield to ultimate ratio in high strength steels for use in offshore engineering. 14th International Conference of OMAE, III: 365, 1995.
- [4] Prior F, Maurer KL. Fatigue strength properties of welded joints of high-strength weldable structural. *Materialwissenschaft und Werkstofftechnik* 1995; 26(3): 161-171.
- [5] Agerskov H, Petersen RI. An investigation on fatigue in high-strength steel offshore structures. *Welding in the World* 1997; 41(4): 328-342.
- [6] Petersen RI, Agerskov H, and Lopez ML. Fatigue life of high strength steel offshore tubular joints. Report of Technical University of Denmark, Denmark, 1996.
- [7] Sharp JV, Billingham J, Stacey A. Performance of high strength steel used in jack-ups. *Marine Structures* 12(1999): 349-370.
- [8] Stacey A, Sharp JV, and King RN. High strength steels used in offshore installations. *International Conference of OMAE Volume III*: 417-433, 1996.
- [9] Etube LS. Fatigue and fracture mechanics of offshore structures. London and Bury St Edmunds, UK, Professional Engineering Publishing Limited, 2001.
- [10] Chen H. Fatigue resistance of high performance steel (HPS) details. Ph.D. Thesis: University of Alberta, Edmonton, Alberta, Canada, 2005.
- [11] Maddox SJ. Fatigue strength of welded structures (second edition). Abington Publishing, Woodhead Publishing Ltd, Abington Hall, England, 1991.
- [12] Anami K, Miki C. Fatigue strength of welded joints made of high-strength steels.

Progress in Structural Engineering and Materials, 2001(3): 86-94.

- [13] Miki C, Homma K, Tominaga T. High strength and high performance steels and their use in bridge structures. *Journal of Constructional Steel Research*, 58(2002): 3-20.
- [14] Ikeda K, Kihara S. Brittle fracture strength of welded joints. *Welding Journal* 1970; 49(3): 106-114.
- [15] Stacey A, Barthelemy JY, Leggatt RH, Ainsworth RA. Incorporation of residual stresses into the SINTAP defect assessment procedure. *Engineering Fracture Mechanics* 2000; 67(6): 573-611.
- [16] Billingham J, Sharp JV, Spurrier J, and Kilgallon PJ. Review of the performance of high strength steels used offshore. *Research Report 105, Health & Safety Executive, Bedfordshire, UK, 2003.*
- [17] Bjorhovde R. Development and use of high performance steel. *Journal of Constructional Steel Research*, 60(2004): 393-400.
- [18] Masubuchi K, Martin DC. Investigation of residual stresses by use of hydrogen cracking. *Welding Journal* 1966; 40(12): 553-563.
- [19] Masubuchi K. *Analysis of welded structures. Residual stresses, Distortion, and their Consequences.* Pergamon Press. Oxford, 1980.
- [20] Lee HY, Biglari FR, Wimpory R, Nikbin KM. Treatment of residual stress in failure assessment of procedure. *Engineering Fracture Mechanics*, 2006; 73(13): 1755-1771.
- [21] Acevedo C and Nussbaumer A. Residual stress examination of welded tubular K-joints under fatigue loads. 12th International Conference on Fracture. Ottawa, 2009.
- [22] ASTM E837-08. *Standard Test Method for Determining Residual Stresses by Hole-Drilling Strain-Gage Method.* ASTM International, West Conshohocken, PA 19428-2959, United States, 2008.
- [23] Lee CK, Chiew SP, Jiang Jin, Residual stress study of welded high strength steel plate-to-plate joints, Part 2: Numerical modeling and parametric study, Accepted by *Thin-walled Structures*
- [24] Corus Construction & Industrial. RQT701 Data Sheet, Scunthorpe, North Lincolnshire, Britain.2006.
- [25] AWS. ANSI/AWS A5.5. *Specification for Low-Alloy Steel Electrodes for Shield Metal Arc Welding.* American Welding Society, Miami, USA. 2006.

- [26] BSI. BS EN1011-2: Welding-Recommendations for welding of metallic materials- Part 2: Arc welding of ferrite steels, London, UK, British Standards Institute, 2001.
- [27] AWS. AWS D1.1. Structural Welding Code-Steel. American Welding Society, Miami, USA. 2008.
- [28] Law M, Kirstein O, and Luzin V. An assessment of the effect of cutting welded samples on residual stress measurements by chill modeling, *Journal of Strain Analysis*, 45(2010):567-573.

Nomenclature

\bar{a}	Calibration constant for normal stresses
\bar{b}	Calibration constant for shear stresses
D	Gauge circle diameter
D_0	Diameter of the drilled hole
E	Young's modulus
Q	Heat input
l	Weld filler length in the chord plate surface
l_1	The length of the chord plate
l_2	The length of the brace plate
R	Weld root length
T_p	The preheating temperature
t_1	The thickness of the chord plate
t_2	The thickness of the brace plate
α	Clockwise angle from the x-axis to the maximum principle stress
β	End preparation angle for the specimens
ε	Relieved strain due to the hole-drilling
θ	Joint angle
ν	Poisson's ratio
σ_c	Calibration stress
σ_x	Uniform normal stress in x direction
σ_y	Uniform normal stress in y direction
τ_{xy}	Uniform shear stress
σ_1	Maximum principle stress
σ_2	Minimum principle stress
AWS	American Welding Society
CET	Equivalent carbon content
HAZ	Heat affected zone
HSS	High strength steel

Table1 Mechanical properties of RQT701 steel plate and LB-70L electrode

Items	Minimum Yield Strength (MPa)	Tensile Strength (MPa)	Minimum Average Impact Energy	Minimum elongation (%)
RQT701	690	790~930	27J@ -45°C	18
LB-70L	685	755	108J@-60°C	27

Table 2 Chemical composition of the RQT701 steel plate and the LB-70L electrode

CET(%)	C	Si	Mn	S	P	Cr	Mo	V	Ni	Cu	B	Al	Nb	Ti	O
RQT701 Plate	0.14	0.40	1.35	0.003	0.012	0.01	0.12	0.05	0.01	0.01	0.002	0.035	0.035	0.025	/
LB-70L electrode	0.04	0.40	1.28	0.003	0.006	0.04	0.48	0.01	3.65	0.01	/	/	/	/	0.03

Table 3 Geometry of the specimens

θ (°)	β (°)	l_1 (mm)	l_2 (mm)	W (mm)	t_1 (mm)	t_2 (mm)	R (mm)	l (mm)
					8	8	5	16
135	90	440	440	420	12	12	5	22
					16	16	5	28
					8	8	6	20
90	60	440	440	420	12	12	6	27
					16	16	6	35

Note: Width of all specimens = 150mm

Table 4 Welding specification for the specimens

Welding Position	Base Metal	Current	Heat Treatment		Inter-pass Temperature	Welding Parameters		
			Preheat	Without Preheat		Current, I	Voltage, U	Welding speed, v
Flat	RQT701	DCEP	100°C	30°C	150°C	170A	26V	2.6 mm/s

Table 5 Coefficients \bar{a} and \bar{b} at different depths

$d(\text{mm})$	0.25	0.50	0.75	1.00	1.25	1.50	1.75	2.00
d/D	0.05	0.10	0.15	0.20	0.25	0.30	0.35	0.40
\bar{a}	0.031	0.069	0.095	0.121	0.118	0.142	0.142	0.149
\bar{b}	0.034	0.112	0.157	0.199	0.227	0.326	0.304	0.360

Table 6 Residual stress measurement results

Specimen Cases				Stress in the measuring points (MPa) (-ve for compressive stress)						
θ ($^{\circ}$)	t (mm)	Preheating	Brace Plate Cutting	A	B	B_1	B_2	B_3	C	
90	8	Yes	Yes	-	-66.2	76.4	25.2	8.0	-	
		No		-	-70.3	129.0	28.2	28.5	-	
	12	Yes		-	-32.5	34.6	11.2	6.2	-	
		No		-	-8.8	67.5	26.9	5.3	-	
	16	Yes		-	51.1	91.9	25.2	5.2	-	
		No		-	24.9	52.4	38.2	-26.4	-	
	8	Yes	No	-	38.2	75.5	-16.0	-18.0	-	
		No		-	110.1	60.8	65.7	-32.2	-	
		12		Yes	-	59.3	42.4	-46.2	-20.4	-
				No	-	87.2	62.5	11.0	-42.6	-
		16		Yes	-	96.3	58.9	29.1	-6.3	-
				No	-	115.5	86.5	20.7	-18.3	-
135	8	Yes	No	-78.8	119.1	99.2	118	-	42.6	
		No		23.2	151	96	90.9	-	-25.6	
	12	Yes		-82.4	62.8	48.5	36.9	-	-68.2	
		No		-15.6	102.6	79.7	32.3	-	-42.7	
	16	Yes		47.7	132.8	114.9	53.4	-	16	
		No		12	213.6	103.9	68.1	-	-68.5	

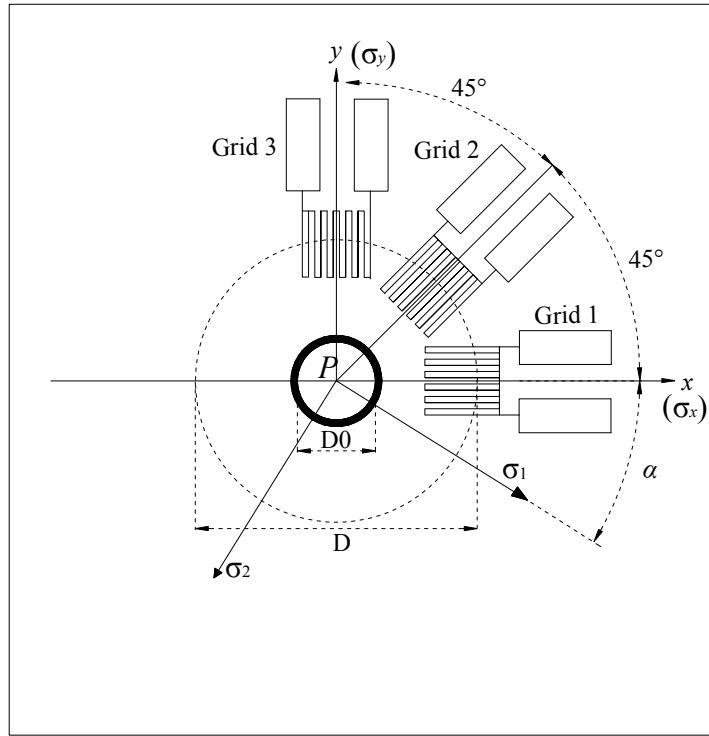


Fig. 1 Schematic diagram of strain gauge for residual stress measurement at point P

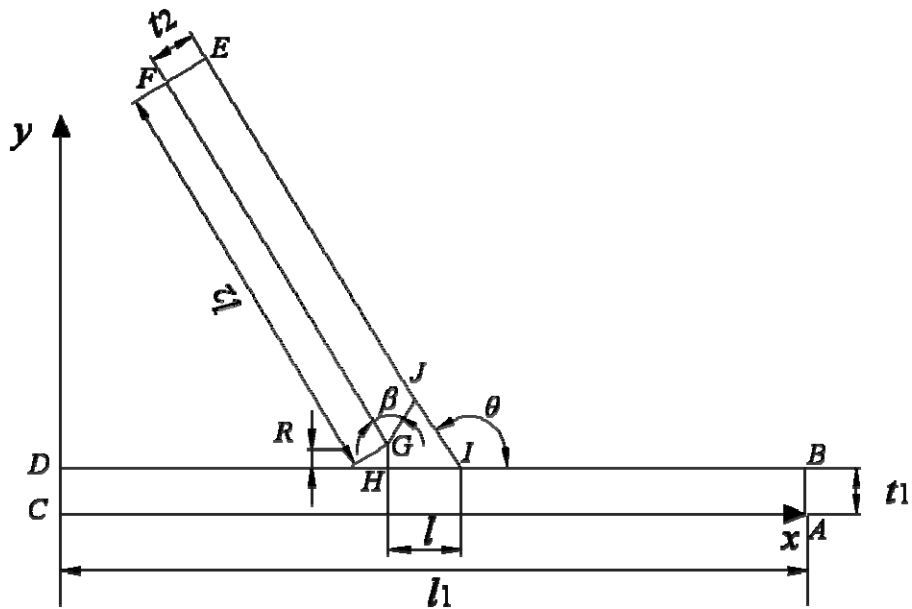


Fig. 2 Typical welding profile of plate-to-plate joint (for $\theta=90^\circ$ and 135°)

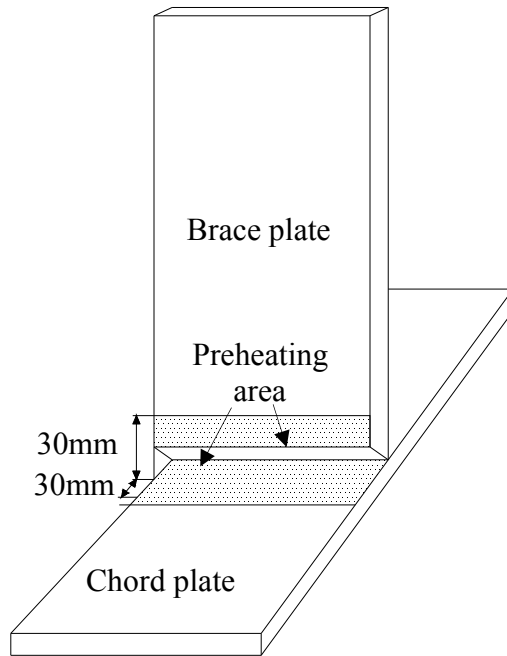


Fig. 3 The preheating area



Fig. 4 The preheating process

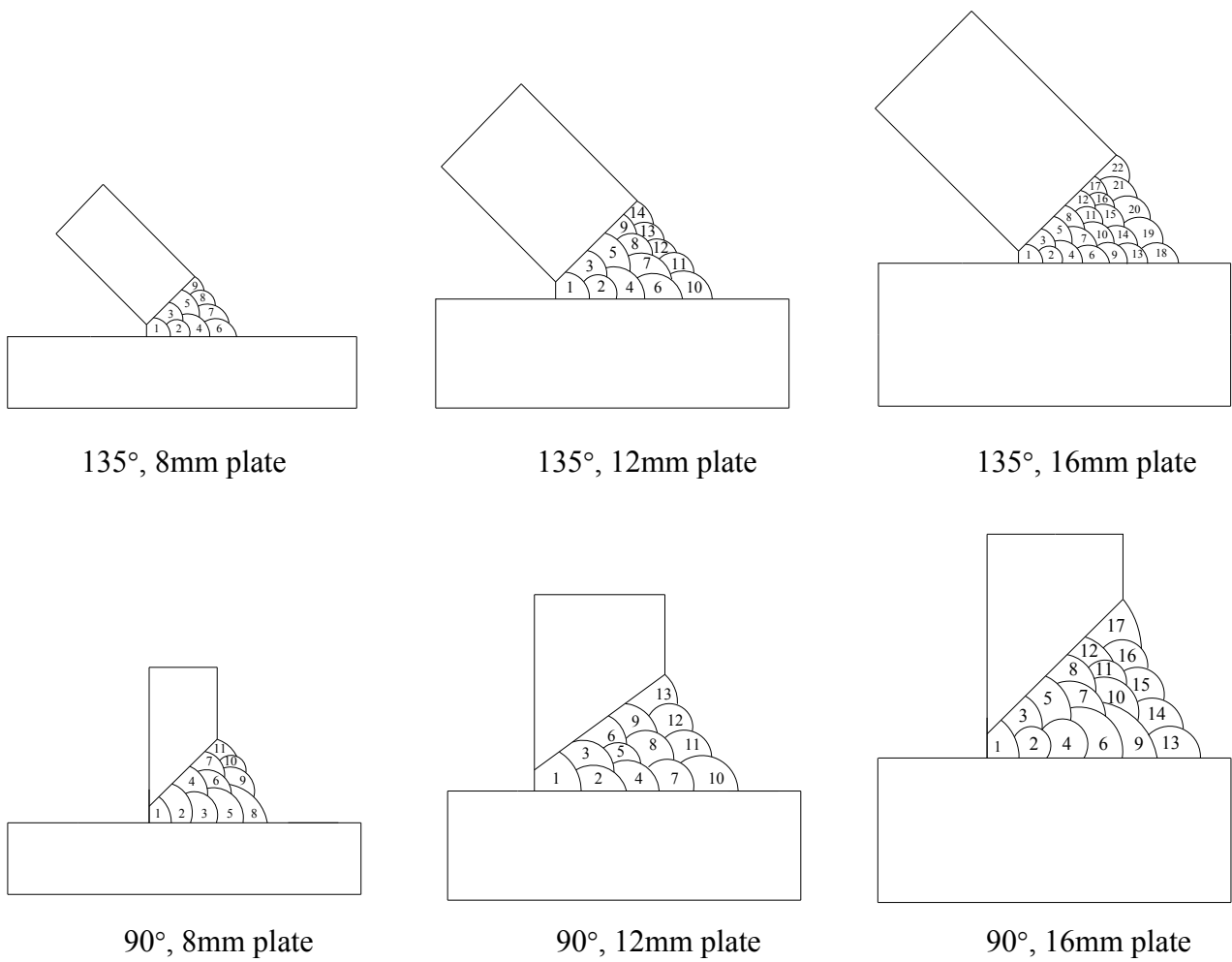
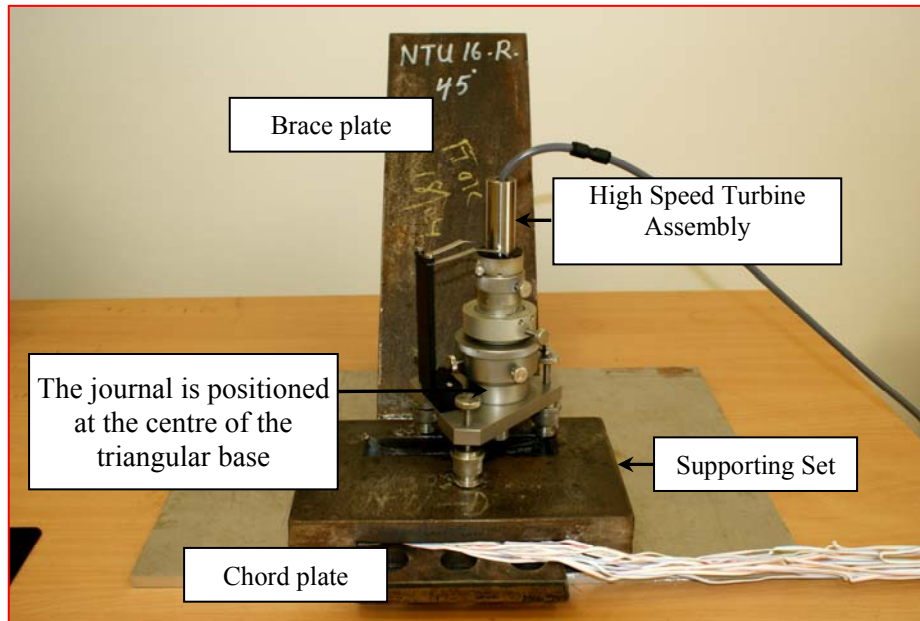
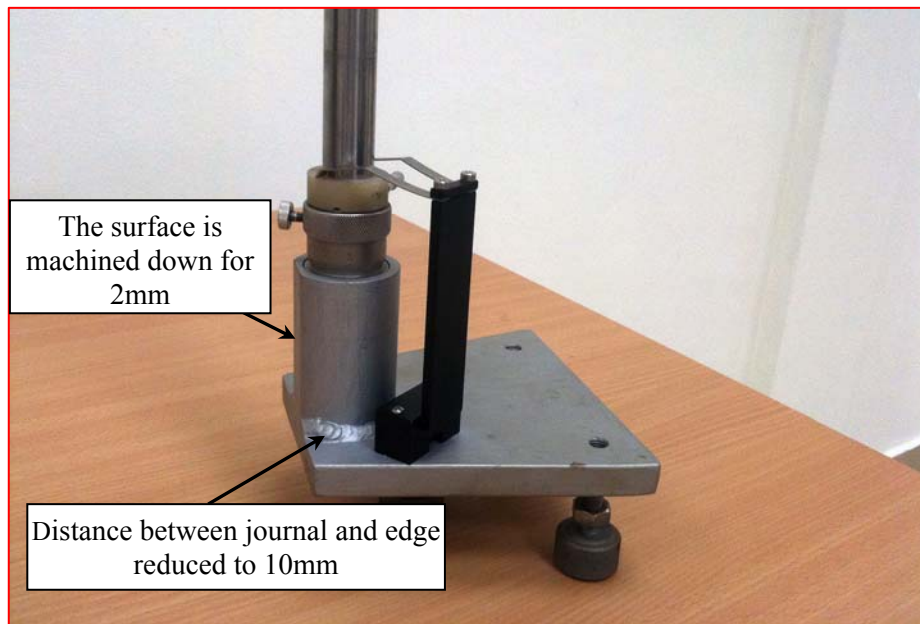


Fig. 5 The number of welding passes and welding sequences adopted for joints with different thickness and intersection angles



(a) The original milling



(b) The revised milling guide

Fig. 6. The RS-milling guide for residual stress measurement

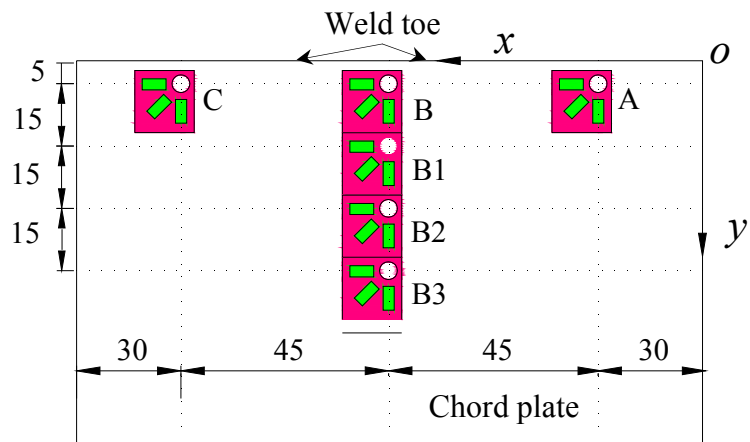


Fig. 7 Strain gauge locations on chord plate for residual stress measurement
(All dimensions in mm)

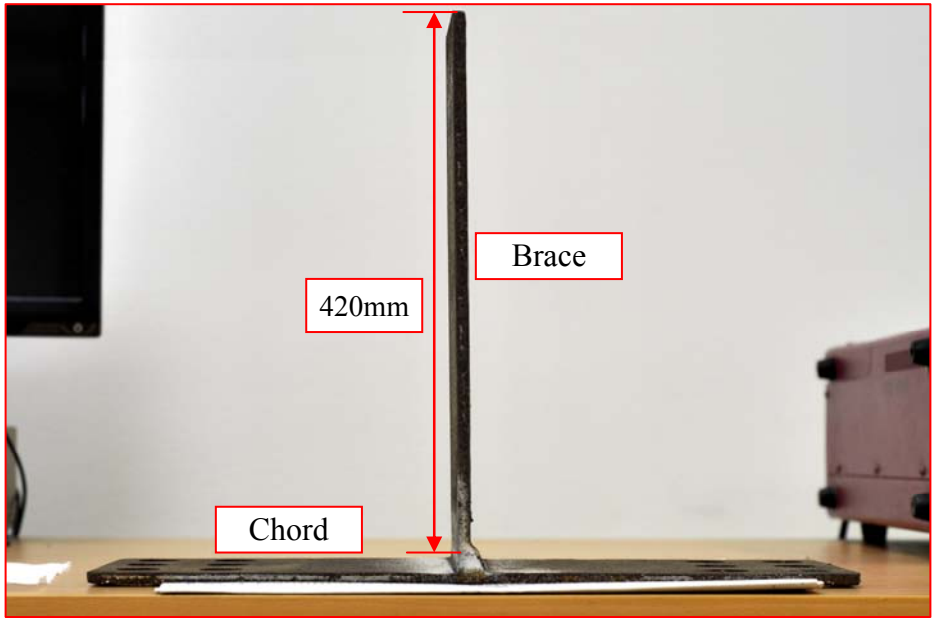


Fig. 8 A T-joint before cutting of the brace plate

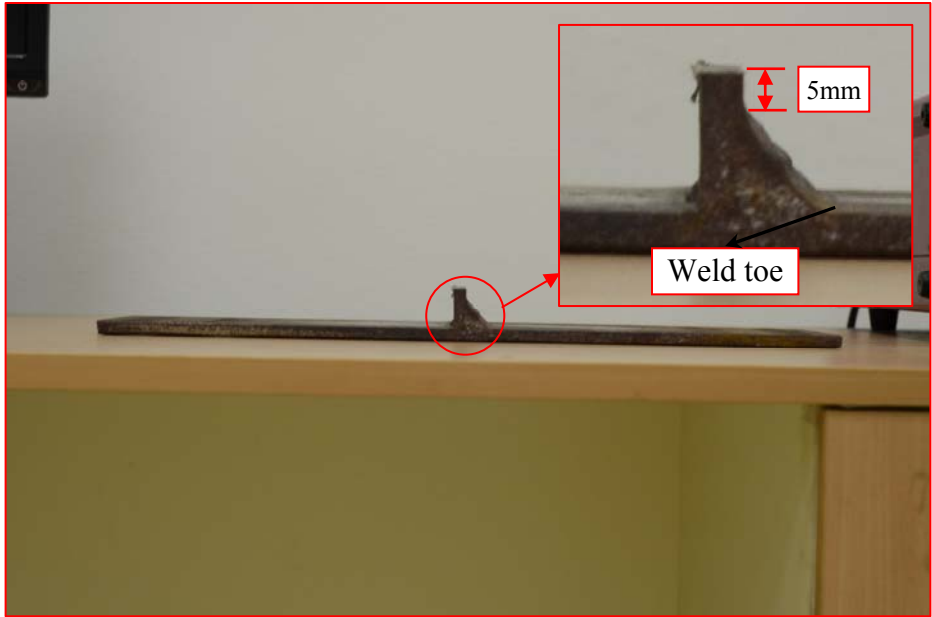


Fig. 9 A T-joint after cutting of the brace plate

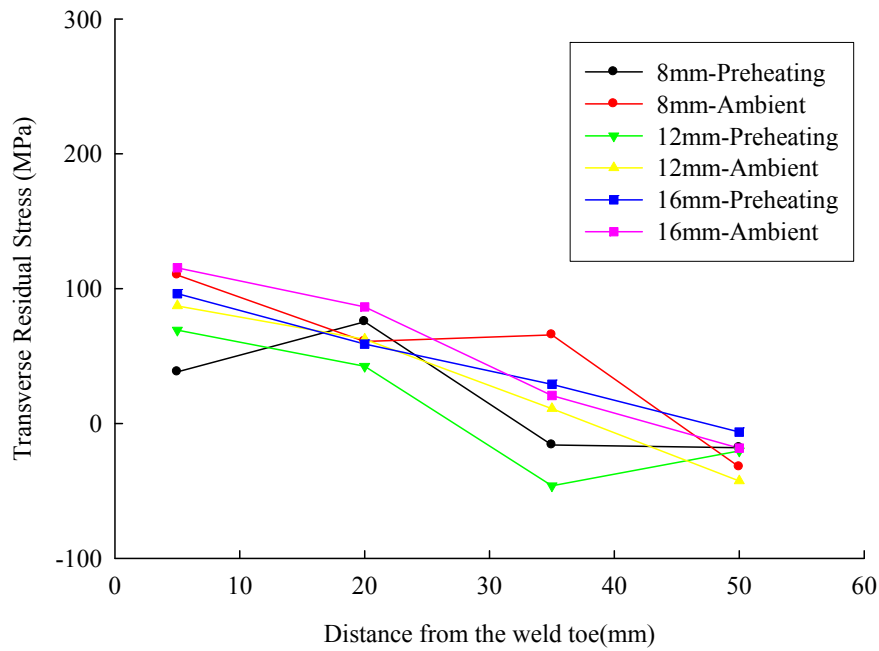


Fig. 10 Residual stresses distribution along the transverse direction (y axis, gauges B, B1, B2 and B3) for 90° joints

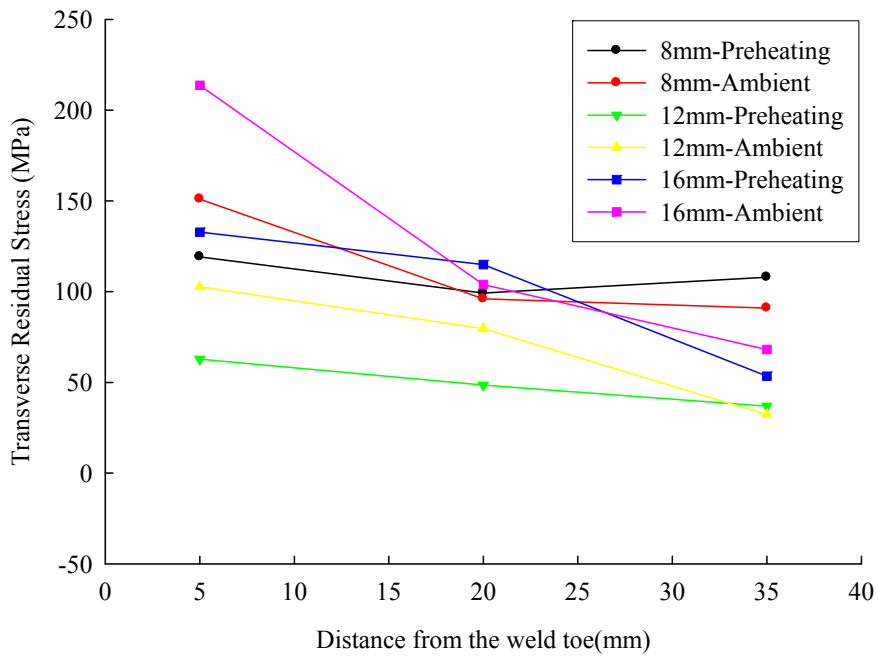


Fig. 11 Residual stresses distribution along the transverse direction (y axis, gauges B, B1 and B2) for 135° joints

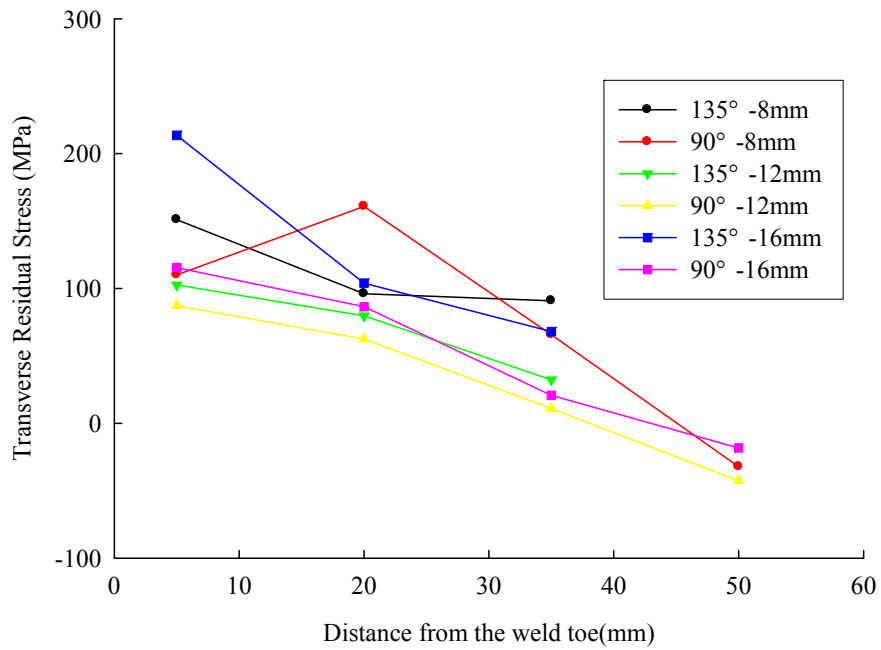


Fig. 12 Residual stresses distribution along the transverse direction (y axis) for joints welded at ambient temperature

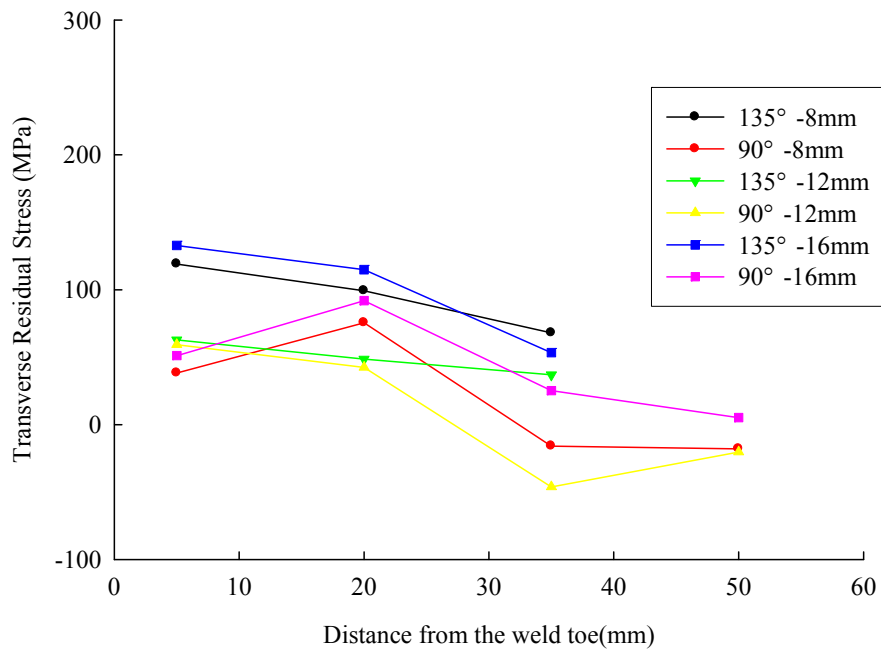


Fig. 13 Residual stresses distribution along the transverse direction (y axis) for joints with preheating

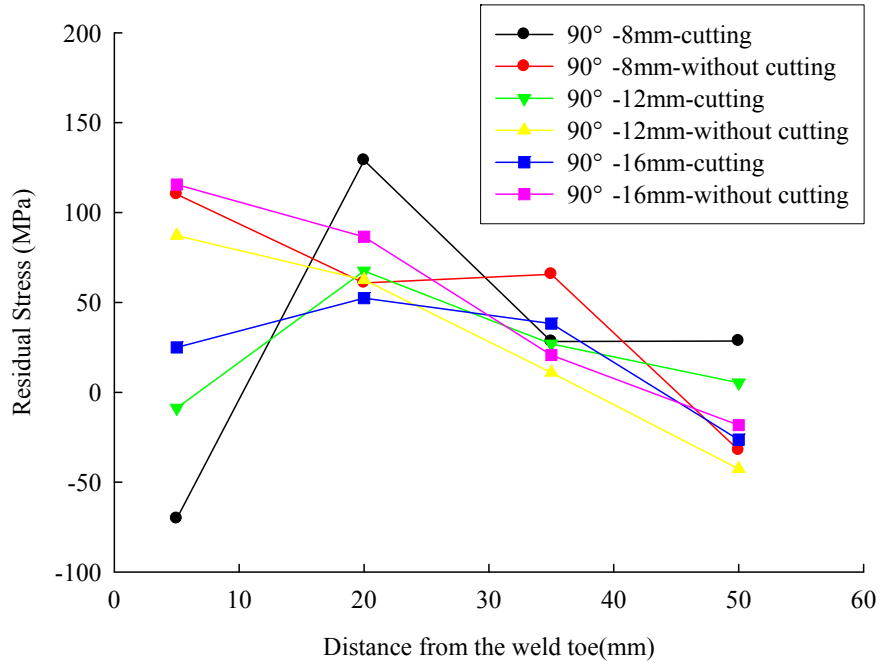


Fig. 14 Effects of brace plate cutting for 90° joints welded at ambient temperature

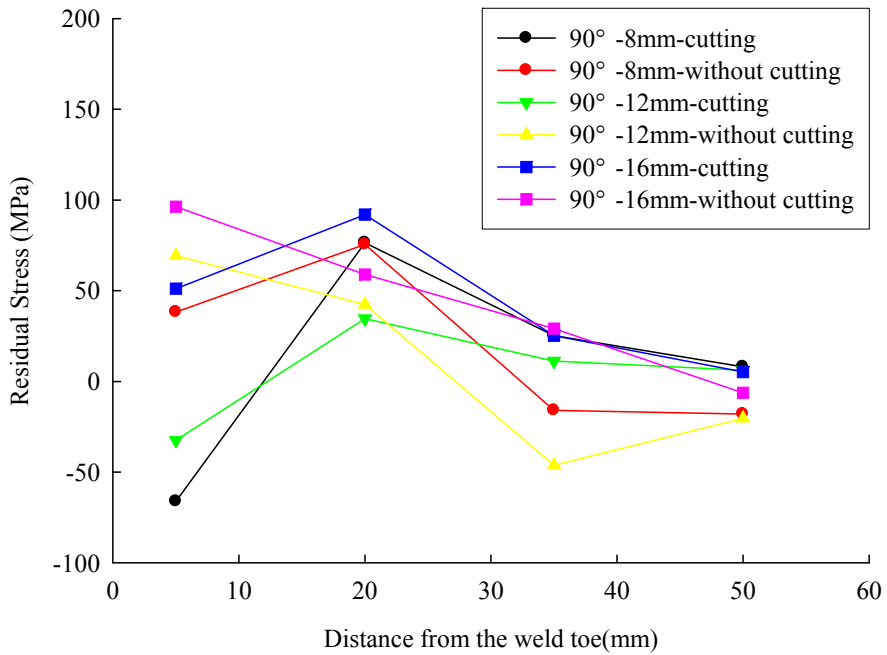


Fig. 15 Effects of brace cutting for 90° joints with preheating

